Growth and Characterization of ZnO Nanorods Prepared by Chemical Bath Deposition for Dye-Sensitized Solar Cell Photoanodes

Noor A. Abdullah, Basil A. Abdullah*and Manal Z. Rajab

Department of Physics, College of Science , University of Basrah, Basrah, Iraq.

***Corresponding author E-mail:** basil.abdullah@uobasrah.edu.iq

https://doi.org/10.29072/basjs.20260117

ARTICLE INFO

Received: 11 December 2025

Accepted: 23 April 2026

Published: 30 April 2026

Keywords:

Chemical Bath Deposition (CBD), DSSCs, ZnO nanorods (NRs), ZnO nanostructure

ABSTRACT

Chemical bath deposition (CBD) was used effectively to create zinc oxide (ZnO) nanorods (NRs) on fluorine-doped tin oxide (FTO) substrates, which were then used as photoanodes in dye-sensitized solar cells (DSSCs). The production of a Wurtzite-type hexagonal crystalline phase with a preferential orientation along the (002) plane was confirmed by structural characterization using X-ray diffraction (XRD). Field-emission scanning electron microscopy (FE-SEM) revealed vertically aligned nanorods with uniform morphology. Optical analysis via UV-Vis spectroscopy indicated reduced band gap of (3.27) eV and high transparency in the visible spectrum compared to bulk ZnO. The fabricated DSSCs based on these ZnO (NRs) Photoanodes exhibited under air mass (AM 1.5G) solar illumination simulation, the photocurrent density (Jsc) was 0.911 mA/cm², the filling factor (FF) was 29%, the open circuit voltage (Voc) was 0.27 V, and the power conversion efficiency (PCE) was 0.07%. These results suggest that ZnO nanorods preparation via CBD present a promising low-cost alternative for DSSC photoanodes.

1. Introduction

Many scholars are interested in the chemical bath deposition (CBD) method for producing zinc oxide nanostructures due to its tunable optical characteristics, low cost of manufacturing, and wide range of applications in optoelectronics, sensors, and photocatalysis. Band gap,

transmittance, photoluminescence, absorption, and other fundamental optical properties are all greatly influenced by the shape, crystallisation, and distribution of defects, which may be greatly controlled using the CBD approach. A recent study has empirically demonstrated how the spectral response of ZnO nanorod, nanowire, and thin films can be fabricated in a controlled manner by systematic variation of compositional parameters, namely: the precursor concentration; the growth temperature; solution pH, the seed layer properties, and the type of dopant involved. Some methods which lead to better crystallinity and aspect ratio often lead to both better transmittance and better tunability of the band gap[1-4].

Currently, Photovoltaic cells are devices that convert light into electrical energy. Among the various available commercial solar cells, dye-sensitized solar cells (DSSCs) have gained significant interest in recent years due to their key advantages and potential functions, which include increasing efficiency and lowering manufacturing costs [5-10]. Michael Gratzel and Brian O Regan have been the first ones to suggest such Solar cells based on sensitizers DSSCs in the year 1991 [11]. Research is increasing on improving the stability of DSSCs to enhance the performance of their constituent materials. Low efficiency and expenses to operate Substrates, ruthenium dye and platinum are some of the weaknesses of DSSCs that have to be substantially enhanced. The role of photoanodes in DSSCs can not be underestimated as they provide a surface onto which the dye hole is held and through which the photo-generated electrons are transported to the external circuits [12]. Semiconductors have attracted a lot of research because of their wide applicability in several areas. There are many kinds of semiconductors; they include Titanium dioxide TiO_2, Zinc oxide ZnO, Cerium dioxide CeO_2 etc. [13-21]

The effective conversion of photon energy into electrical power depends on the large surface area of porous nanocrystalline semiconductor oxide sheets for the adsorption of dye molecules. A photoanode must have a sufficient surface area, remarkable electron transport properties, and a low rate of electron and hole recombination in order to achieve premium functions [22, 23]. However, zinc oxide is considered one of the preferred materials in the preparation of the photoanode in the development of DSSCs, where the electron mobility is large and also relative to fewer surface states (recombination centers), bearing in mind that it has high potential and considerable properties of ZnO. Pooja B. More et al. used a CBD technique to create ZnO thin films on FTO substrate. The thin films' rod-like shape and hexagonal wurtzite structure had an average width of 340 nm and height of 630 nm. With an

optical energy gap of 3.1 eV and a charge carrier density of 8.5×10^{18} cm^3, the electrochemical test confirmed n-type conductivity. [24]. Büşra Altun and colleagues investigated the effects of cobalt doping on ZnO thin-film sensors, specifically looking at their optical, structural, and CO_2 gas sensing characteristics. They achieved the doping by incorporating (1%, 3%, 5%, and 7%) cadmium through using CBD. Notably, the sensor doped with 3% cadmium exhibited the most significant CO_2 response, along with rapid response times, excellent selectivity, and remarkable stability [25]. Hunge Y. M. et al reported well-aligned ZnO (NRs) with varying reaction times in CBD method for the application of photo catalysis [26]

In this work, ZnO (NRs) will be deposited on FTO substrates using CBD, and various measurements will be used to examine the impact of this process on the morphological, optical, and structural characteristics of the ZnO (NRs). With the intention of applying the material to DSSCs, XRD, FE-SEM, UV-vis spectroscopy, and room temperature photocurrent measurement have been employed.

2. Materials and Methods

2.1. FTO substrate cleaning

The FTO layer was cut using a diamond cutter to obtain a smaller substrate. They were then cleaned in an ultrasonic bath with acetone, ethanol, and deionized water for 10 minutes, respectively. The samples were then left to dry at 50 °C for 30 minutes. The purpose of substrate cleaning is to avoid pollution by any other impurity.

2.2 Synthesis of ZnO (NRs) by CBD Growth

(CBD) consists of a two-step on FTO glass seeding and solution growth process):

2.2.1 First step (Preparing the ZnO seed layer)

The ZnO seed layer was created by dissolving 5 mM zinc acetate dihydrate ($Zn(CH_3CO_2)_2 \cdot 2H_2O$) in 50 ml of ethanol while stirring for three hours at room temperature. After cleaning the glass substrates, the seed solution was spin-coated and thermally dried at 50 °C. In order to eliminate the solvent and guarantee nucleation, these seeded substrates were further annealed at 350 °C for one hour in an air atmosphere before being allowed to cool to room temperature[27].

2.2.2 Second step (Growth of ZnO nanorods)

(CBD) has been used to grow ZnO epitaxial (NRs) on a seeded glass substrate. The growth solutions were prepared by dissolving separately (0.1 M) Zn $(NO_3)_{26}H_2O$ and $C_6H_{12}N_4$ in (25 ml) of distilled water (DW) to a temperature of (70°C). The two solutions were then mixed, and the seeded substrates were dipped vertically in a beaker set at a temperature of (90°C) and left to soak in the solution at (90°C), within 2 h. Samples after growth were taken out of the solution and washed successively in DW and ethanol, dried, and treated at (350°C) for 1 h. As shown in Table 1 .[27, 28].

Table 1. Summary of the Experimental Steps

Step (1)	**Zinc acetate dihydrate (5mM) + (50ml) ethanol**	➡	**Coating (at T50°C) 10 layers (FTO) / 50s each+ annealing (1h/350°C)**	➡	**Seed Layer**
Step (2)	(0.1 M) for each (zinc nitrate hexahydrate + hexamethylenetetramine +(25ml) H_2O	➡	Coating (at 90°C) for (3 h) + Post-annealing (1h/350°C)	➡	Nanorods grown (NRs)

2.3 Fabrication of DSSCs.

Sensitization of a set of ZnO nanorod-coated fluorine-doped tin oxide (FTO) substrates was done by immersion in the room temperature (0.5 mM) sensitizer solution for 24 h. As counter electrode a Pt foil (150 µm) was used. The FTO electrode coated with the ZnO nanorod was put together with the counter electrode, and its combination was sealed with a Parafilm spacer at a thickness (25 µm). In order to enable dye regeneration under oxidizing circumstances, 0.127 g of iodine (I2) and 0.83 g of potassium iodide (KI) were dissolved in 10 mL of ethylene glycol to create the redox mediator [29]. Its solar cell performance was defined through capturing of its respective current-voltage (I-V) pattern under illumination by (1.5Am) type of simulated sunlight. The area of the cell was (0.3×0.3) cm². The conversion efficiency of power was then determined according to [30]:

$$\eta = \frac{V_{oc} \times F.F}{P_{in}} \qquad (1)$$

And the filling factor (F. F) is defined:

$$\mathrm{F.F} = \frac{V_{max}\ x\ I_{max}}{V_{oc}\ x\ I_{sc}} \qquad (2)$$

Where: Pin: the intensity of the incident light.

V_{oc}: the open-circuit voltage (mV)

I_{sc}: stands for short circuit current density.

I_{max}, V_{max}: current, voltage at maximum power output, respectively

3. Results

3.1 XRD Diffraction

The XRD analysis (Fig. 1) proved the crystalline status of ZnO having a hexagonal structure of wurtzite (JCPDS Card No. 65-3411) and lattice a = 3.249 A°, c = 5.206 A°. The diffraction peaks of the 2θ angles are 31.8, 34.4, 36.3, 47.5, 56.6, 62.8 and 67.9 that corresponding to the (100), (002), (101), (102), (110), (103), and (112) planes respectively. The (002) orientation is high hence the peak at 34.4 is strong. The Scherrer equation was used to calculate the dimensions of the average crystallite which is 42.29 nm [31]:

$$\mathrm{D} = \frac{0.9\,\lambda}{\beta\cos(\theta)} \qquad (3)$$

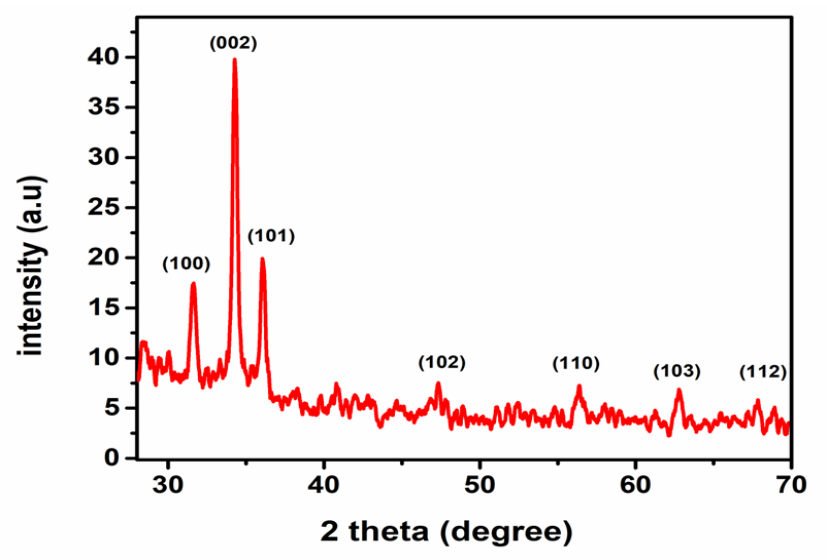

Figure 1. XRD pattern of ZnO (NRs) grown by CBD.

3.2 Surface Morphology Analysis

According to the view of the FESEM (Fig. 2), ZnO nanorods exhibits well-aligned hexagonal morphology, which is essentially vertical standing on the substrate surface. It is clear from the image micrographs that the ZnO film indicates that rod-like structure [32]. The ImageJ software was used to measure the average diameter of the (NRs) which measured to be in the range of (80-150 nm).

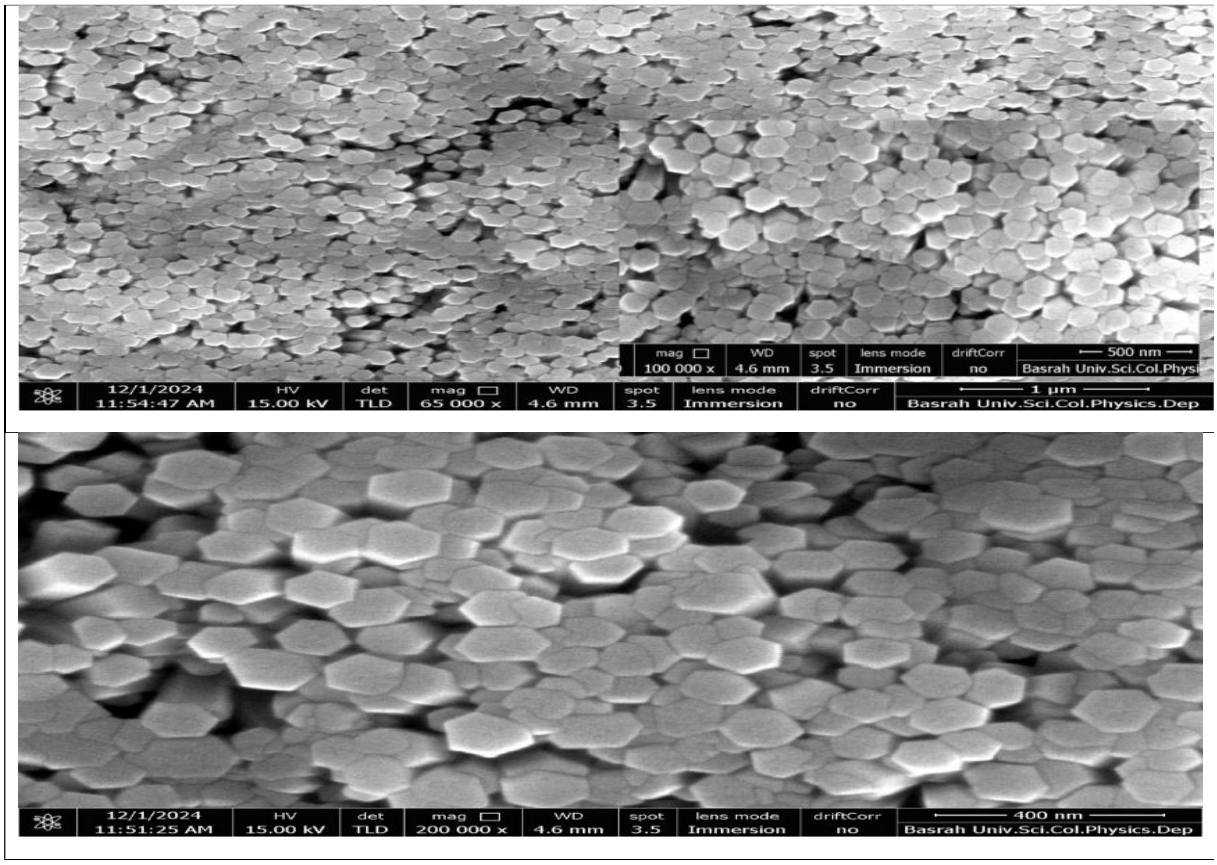

Figure 2. FESEM images of ZnO (NRs) grown by CBD

3.3 Optical Analysis

In Fig. 3(a), UV-Vis absorbance intensity range of (300-800 nm) spectral range of the ZnO (NRs) obtained by CBD process is shown. The spectra show a region of peak absorption of 385 nm; this is attributed to electronic transitions between valence band and conduction band (O2p -Zn3d) that happens with the band gap and peak of absorbance that is characteristic of ZnO [33, 34]. Figure 3(b) represents the calculated band gap of ZnO (NRs) as obtained in the UV-Vis. spectrum which is found to be (3.27 eV). Crystalline

ZnO crystals usually follow the crystal structure of wurtzite, are direct band gap-type material (3.33 eV) [35]. The variances in optical bandgap that can be observed can be explained by the scattering that happens at grain boundaries and results in the marginal shift of the optical absorption edge that is shifted towards higher wavelength. The consequence of this shift is that, it causes a decrease in the energy bandgap of the material [36,37]. Also, the energy bandgap of the films can drop slightly due to formation of oxygen vacancies in the films [38].

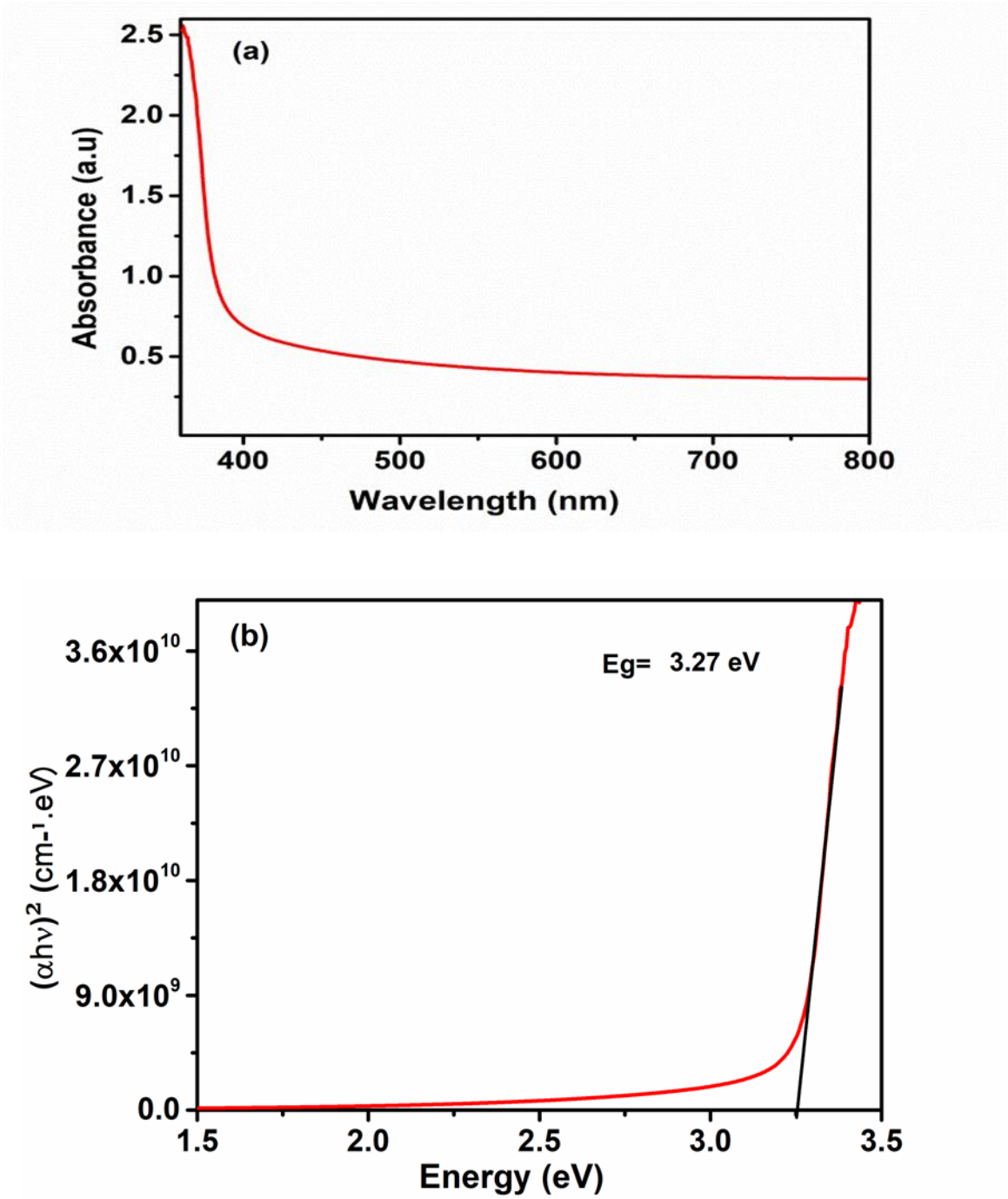

Figure 3. (a) UV absorbance Spectrum , (b) Tauc plot of ZnO (NRs) grown by CBD.

4. Discussion

4.1 J – V Analysis

Figure 4. shows the photocurrent density voltage (J-V) characteristic of the CBD-grown ZnO (NRs) photoanode with simulated sunlight (100 mW/cm^2). The device had a low power conversion efficiency (PCE) of 0.07 percent, having a photocurrent density of 0.911 mA/cm^2 with a fill factor (FF) of only 29%. An exceptionally low FF is one of the key indicators of important charge recombination losses. It is not isolated to ZnO-based DSSCs which have a reputed high density of surface defects and trap states that facilitate rapid electron recombination [39]. Moreover, the lack of a dense blocking material at the FTO/ZnO interface could also be a cause of back electron transfer to the electrolyte, which subsequently decreases the open-circuit voltage and fill factor.

The reduced photocurrent density may be explained by the defects in dye-sensitization process. Solvation of the ZnO surface by the carboxylates of the dye may cause complexation of the dyes with Zn^{2+} or even partial dye degradation and thus reducing the actual dye loading and light-harvesting efficiency [40]. This, together with the natural charge recombination, entirely explains the low overall efficiency that is apparent in this unoptimized system. Power conversion efficiencies (PCEs) of Zinc oxide-based (DSSCs) and (PSCs), are typically (less than one percent) in poorly optimized, poorly-engineered, defect-prone non-nanostructured photoanodes, and (between three and six percent) in more carefully prepared, nanostructured photoanodes. Moreover, higher-order perovskite structures that include the design of engineered electron transport layers have shown efficiencies of more than (20 %) [41,42]. An example of this is the combination of zinc oxide nanotetrapods to facilitate DSSCs, which have reported better efficiencies that exceeding (3) % ,whereas composite photoanodes (zinc oxide and tin oxide) can achieve better efficiencies that exceeding (6) % under ideal conditions; though, their functionality is required to include multilayer designs and severe control of absorption layer thickness [43]. zinc oxide/cadmium sulfide/cadmium telluride thin-film solar cells can theoretically achieve efficiencies of more than (20)[44].

Moreover, ZnO is also an alloy with a greatly high concentration of surface defects and trap states, which are prone to fast electron recombination and slow charge transport. The lack of an efficient compact or blocking layer between the ZnO and conducting substrate

also contributes to the back electron transfer, sacrificing the open-circuit voltage and fill factor [39].

Abel Garcia-Barrientos et al reported that the pH level used in the process of growing the film of ZnO has an extreme influence on the crystalline quality of the film. This, in its turn, has a direct effect on the efficiency of the solar cell [45]. Moreover, morphology of the nanorods (length and density) and sensitization conditions (solvent, pH and possible dye aggregation) are very vital in defining the dye adsorption and hence the overall photovoltaic performance. All these facts explain why efficiency of ZnO-based DSSCs is low in comparison with the TiO_2 counterparts. The variables that should be controlled in order to maximize the CBD method include growth time and concentrations of precursors. This helps in reducing defects and produce well aligned nanorods which improve performance [46, 47].

Table 2. Photovoltaic characteristics of ZnO (NRs) DSSCs grown by the (CBD) under solar illumination (100 mW/cm^2).

V_{oc} (V)	J_{sc} (mA/cm^2)	V_m(V)	F.F (%)	η (%)
0.27	**0.911**	**0.11**	**29**	**0.07**

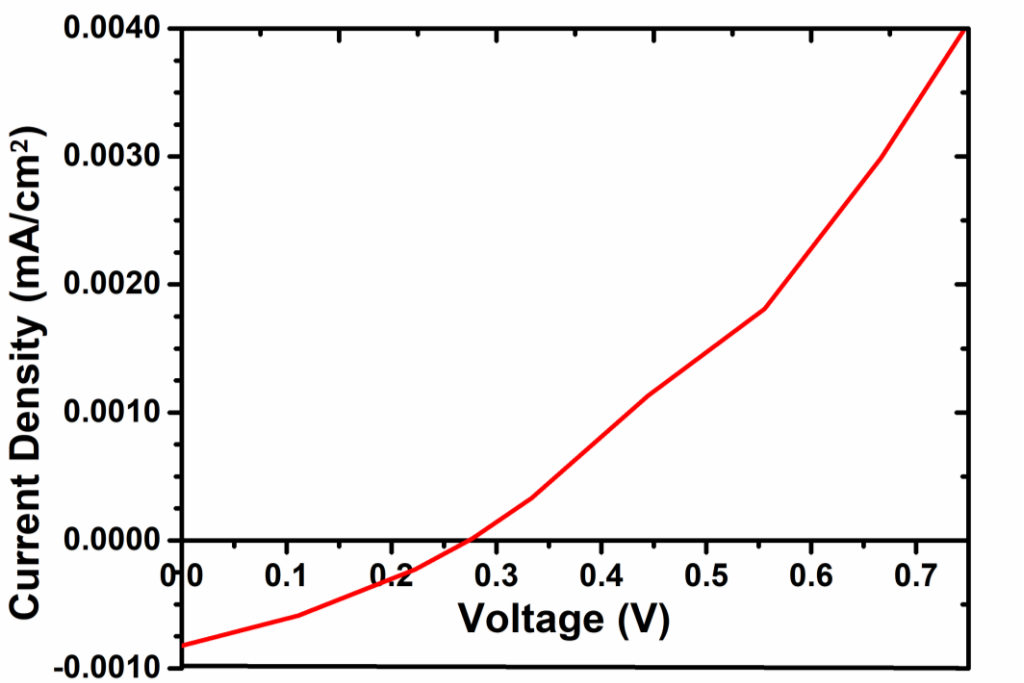

Figure 4.J-V characteristics of ZnO (NRs) DSSCs

5. Conclusions

ZnO films were successfully synthesised in this study employing a straightforward and inexpensive (CBD) approach. At room temperature, structural, morphological, and UV-vis spectroscopic studies were examined. In addition to vertically orientated growth on the FTO substrate, the ZnO XRD pattern showed texturing and a hexagonal wurtzite structure in the (002) direction. Further, the fabrication of a rod structure was confirmed by the FESEM results. ZnO optical bandgap energy was determined to be 3.27 eV. Finally, these ZnO (NRs) films were used to fabricate (DSSCs) by using them as photoanode materials. Photocurrent intensity measurements showed that, for the deposition methods employed, the presence of a seed layer increased the filling factor but decreased the short-circuit current density. A photo conversion efficiency of 0.07% percent was attained by applying ZnO (NRs) to glass substrates coated with FTO and immersing the resultant photoanode in a ruthenium-based dye solution for 24 hours.

Authors contributions

All Authors have been contributed to the experimental setup, experimental work, data analysis, interpretation, and manuscript preparation. Authors reviewed and approved the final version of the manuscript.

References

[1] K. Mosalagae, D. M. Murape, and L. M. Lepodise, "Effects of growth conditions on properties of CBD synthesized ZnO nanorods grown on ultrasonic spray pyrolysis deposited ZnO seed layers," *Heliyon*, vol. 6, no. 6, p. e04458, 2020, https://doi.org/10.1016/j.heliyon.2020.e04458.

[2] S. Kumar, R. Seth, S. Panwar, K. K. Goyal, V. Kumar, and R. K. Choubey, "Morphological and Optical Studies of ZnO-Silica Nanocomposite Thin Films Synthesized by Time Dependent CBD," *Journal of Electronic Materials*, vol. 50, pp. 3462–3470, 2021, https://doi.org/10.1007/s11664-021-08863-2.

[3] M. Shaban, M. Zayed, and H. S. Hamdy, "Nanostructured ZnO Thin Films for Self-Cleaning Applications," *RSC Advances*, vol. 7, no. 2, pp. 617-631, 2017, https://doi.org/10.1039/C6RA24788A.

[4] M. Patki, R. Bagade, G. Madkaikar, and P. Agarwal, "Study of Surface Morphology and Optical Properties of ZnO Thin Film Synthesized Using CBD Technique," *Journal of Nano- and Electronic Physics*, vol. 12, no. 2, p. 02013, 2020, https://doi.org/10.21272/jnep.12(2).02013.

[5] H. Javed, N. Shahzad, M. A. Khan, M. Ayub, N. Iqbal, M. Hassan, N. Hussain, M. I. Rameel, and M. I. Shahzad, "Effect of ZnO nanostructures on the performance of dye sensitized solar cells," *Solar Energy*, vol. 230, pp. 492-500, 2021, https://doi.org/10.1016/j.solener.2021.10.045.

[6] I. ul Haq, M. I. Khan, M. Irfan, M. Fatima, H. H. Somaily, Z. M. Elqahtani, and N. Alwadai, "Increase the current density and reduce the defects of ZnO by modification of the band gap edges with Cu ions implantation for efficient, flexible dye-sensitized solar cells (FDSSCs)," *Ceramics International*, vol. 49, no. 18, pp. 29622-29629, 2023, https://doi.org/10.1016/j.ceramint.2023.06.188.

[7] F. Yuliasari, A. Aprilia, and R. Hidayat, "Improved dye-sensitized solar cell performance with hedgehog-like shaped ZnO nanorods grown using ZnO nanoparticles seed layer," *Materials Today: Proceedings*, vol. 52, pp. 248–251, 2022, https://doi.org/10.1016/j.matpr.2022.02.193.

[8] K. Jayanthi, S. Chawla, K. N. Sood, M. Chhibara, and S. Singh, "Dopant induced morphology changes in ZnO nanocrystals," *Applied Surface Science*, vol. 255, no. 11, pp. 5869-5875, 2009, https://doi.org/10.1016/j.apsusc.2009.01.032.

[9] A. Derri, M. Guezzoul, A. Mokadem, A. Ouerdane, K. B. Bensassi, M. Bouslama, B. Kharroubi, and E. Hameurlaine, "Insight into the photoluminescence and morphological characteristics of transition metals (TM = Mn, Ni, Co, Cu)-doped ZnO semiconductor: a comparative study," *Optical Materials*, vol. 145, p. 114467, 2023, https://doi.org/10.1016/j.optmat.2023.114467.

[10] O. Muktaridha, A. Adlim, S. Suhendrayatna, and I. Ismail, "Progress of 3d metal-doped zinc oxide nanoparticles and the photocatalytic properties," *Arabian Journal of Chemistry*, vol. 14, no. 7, p. 103175, 2021, https://doi.org/10.1016/j.arabjc.2021.103175.

[11] O'Regan and M. Gratzel, "A low-cost, high-efficiency solar cell based on dye-sensitized colloidal TiO2 films," *Nature*, vol. 353, pp. 737–740, 1991, http://dx.doi.org/10.1038/353737a0.

[12] M. Grätzel, "Dye-sensitized solar cells," *Journal of Photochemistry and Photobiology C: Photochemistry Reviews*, vol. 4, no. 2, pp. 145–153, 2003, https://doi.org/10.1016/S1389-5567(03)00026-1.

[13] V. Jagtap, V. S. Kadam, S. R. Jadkar, and H. M. Pathan, "Performance of N3 sensitized titania solar cell under artificial light ambience," *ES Energy & Environment*, vol. 3, pp. 60-67, 2019, http://doi.org/10.30919/esee8c220.

[14] U. Bach, D. Lupo, P. Comte, J. E. Moser, F. Weissörtel, J. Salbeck, H. Spreitzer, and M. Grätzel, "Solid-state dye-sensitized mesoporous TiO2 solar cells with high photon-to-electron conversion efficiencies," *Nature*, vol. 395, pp. 583-585, 1998, http://doi.org/10.1038/26936.

[15] N. Kawade, P. K. Bhujbal, A. T. Supekar, H. M. Pathan, and K. M. Sonawane, "Eosin-Y sensitized tin oxide (SnO2): fabrication and its analysis," *Optik*, vol. 216, p. 164968, 2020, https://doi.org/10.1016/j.ijleo.2020.164968.

[16] S. Chappel and A. Zaban, "Nanoporous SnO2 electrodes for dye-sensitized solar cells: improved cell performance by the synthesis of 18 nm SnO2 colloids," *Solar Energy Materials and Solar Cells*, vol. 71, no. 2, pp. 141-152, 2002, https://doi.org/10.1016/S0927-0248(01)00050-2.

[17] Y. Fukai, Y. Kondo, S. Mori, and E. Suzuki, "Highly efficient dye-sensitized SnO2 solar cells having sufficient electron diffusion length," *Electrochemistry Communications*, vol. 9, no. 6, pp. 1439-1443, 2007, https://doi.org/10.1016/j.elecom.2007.01.054.

[18] M. Quintana, T. Marinado, K. Nonomura, G. Boschloo, and A. Hagfeldt, "Organic chromophore-sensitized ZnO solar cells: Electrolyte-dependent dye desorption and band-edge shifts," *Journal of Photochemistry and Photobiology A: Chemistry*, vol. 202, no. 2-3, pp. 159-163, 2009, https://doi.org/10.1016/j.jphotochem.2008.11.024.

[19] S. K. Kokate, C. V. Jagtap, P. K. Baviskar, S. R. Jadkar, H. M. Pathan, and K. C. Mohite, "CdS sensitized cadmium doped ZnO solar cell: fabrication and characterizations," *Optik*, vol. 157, pp. 628-634, 2018, https://doi.org/10.1016/j.ijleo.2017.11.098.

[20] R. S. Mane, W. J. Lee, H. M. Pathan, and S.-H. Han, "Nanocrystalline TiO2/ZnO thin films: fabrication and application to dye-sensitized solar cells," *The Journal of Physical Chemistry B*, vol. 109, no. 51, pp. 24254-24259, 2005, https://doi.org/10.1021/jp0531560.

[21] S. A. A. R. Sayyed, N. I. Beedri, V. S. Kadam, and H. M. Pathan, "Rose Bengal-sensitized nanocrystalline ceria photoanode for dye-sensitized solar cell application," *Bulletin of Materials Science*, vol. 39, no. 5, pp. 1381-1387, 2016, https://doi.org/10.1007/s12034-016-1279-7.

[22] N. Ali, A. Hussain, R. Ahmed, M. K. Wang, C. Zhao, B. U. Haq, and Y. Q. Fu, "Advances in nanostructured thin film materials for solar cell applications," *Renewable and Sustainable Energy Reviews*, vol. 59, pp. 726–737, 2016, https://doi.org/10.1016/j.rser.2015.12.268.

[23] J. Albero, P. Atienzar, A. Corma, and H. Garcia, "Efficiency Records in Mesoscopic Dye-Sensitized Solar Cells," *The Chemical Record*, vol. 15, no. 4, pp. 803–828, 2015, https://doi.org/10.1002/tcr.201500007.

[24] P. B. More, S. B. Bansode, M. Aleksandrova, S. R. Jadkar, and H. M. Pathan, "Synthesis of ZnO Thin Films Using Chemical Bath and Investigation of Physicochemical Properties," *ES Energy & Environment*, vol. 22, p. 983, 2023, http://dx.doi.org/10.30919/esee983.

[25] B. Altun, I. K. Er, A. O. Çağırtekin, A. Ajjaq, F. Sarf, and S. Acar, "Effect of Cd dopant on structural, optical and CO2 gas sensing properties of ZnO thin film sensors fabricated by chemical bath deposition method," *Applied Physics A*, vol. 127, no. 9, p. 687, 2021, https://doi.org/10.1007/s00339-021-04843-9.

[26] Y. M. Hunge, A. A. Yadav, S. W. Kang, and H. Kim, "Facile synthesis of multitasking composite of Silver nanoparticle with Zinc oxide for 4-nitrophenol reduction, photocatalytic hydrogen production, and 4-chlorophenol degradation," *Journal of Alloys and Compounds*, vol. 928, p. 167133, 2022, https://doi.org/10.1016/j.jallcom.2022.167133.

[27] M. J. Kadhim, M. A. Mahdi, J. J. Hassan, and A. S. Al-Asadi, "Photocatalytic activity and photoelectrochemical properties of Ag/ZnO core/shell nanorods under low-intensity white light irradiation," *Nanotechnology*, vol. 32, no. 19, p. 195706, 2021, https://doi.org/10.1088/1361-6528/abe3b3.

[28] A. Fernández, J. Fan, and A. Cabot, "Highly crystalline hydrothermal ZnO nanowires as photoanodes in DSCs ",*International Journal of Nanotechnology* ,vol. 11, no. 9-11, pp. 747–757, 2014 ,https://doi.org/10.1504/IJNT.2014.063785.

[29] N. A. Abdullah, B. Ali, and J. Hashim, "Study the Effect of TiO2 Nanoparticles in Multilayers of Photoelectrode Prepared by Ball Milling Technique on The Performance of Dye Sensitized Solar Cells (DSSCs)," *Journal of Physics: Conference Series*, vol. 1818, p. 012069, 2021, https://doi.org/10.1088/1742-6596/1818/1/012069.

[30] Q. Zhang, C. S. Dandeneau, X. Zhou, and G. Cao, "ZnO Nanostructures for Dye-Sensitized Solar Cells," *Advanced Materials*, vol. 21, no. 41, pp. 4087–4108, 2009, https://doi.org/10.1002/adma.200803827.

[31] S. Jayswal and R. S. Moirangthem, "Study of surface morphology and optical properties of ZnO thin film," *AIP Conference Proceedings*, vol. 2009, p. 020023, 2018, https://doi.org/10.1063/1.5052092.

[32] N. Zhou, H. Zhu, S. Li, J. Yang, T. Zhao, Y. Li, and Q. H. Xu, "Effect of gold loading on time resolved ps photoluminescence of ZnO," *The Journal of Physical Chemistry C*, vol. 126, no. 38, pp. 16148–16157, 2022, https://doi.org/10.1021/acs.jpcc.7b12463.

[33] L. Lin, H. Yang, and J. A. A. E., "Lutetium-doped ZnO to improve photovoltaic performance: A first-principles study," *ACS Applied Electronic Materials*, vol. 4, no. 12, pp. 6253–6260, 2022, https://doi.org/10.1021/acsaelm.2c01365.

[34] L. Li, Z. Zhang, J. Wang, and P. Yang, "Improving photoelectric performance with hydrogen on Al-doped ZnO," *Materials Chemistry and Physics*, vol. 291, p. 126680, 2022, https://doi.org/10.1016/j.matchemphys.2022.126680.

[35] S. Khadtare, A. S. Bansode, V. L. Mathe, N. K. Shrestha, C. Bathula, S.-H. Han, and H. M. Pathan, "Effect of oxygen plasma treatment on performance of ZnO based dye sensitized solar cells," *Journal of Alloys and Compounds*, vol. 724, pp. 348-352, 2017, https://doi.org/10.1016/j.jallcom.2017.07.013.

[36] A. Amala Rani and S. Ernest, "Structural, morphological, optical and compositional characterization of spray deposited Ga doped ZnO thin film for Dye-Sensitized Solar Cell application," *Superlattices and Microstructures*, vol. 75, pp. 398-408, 2014, https://doi.org/10.1016/j.spmi.2014.07.048.

[37] S. A. Ansari, M. M. Khan, S. Kalathil, A. Nisar, J. Lee, and M. H. Cho, "Oxygen vacancy induced band gap narrowing of ZnO nanostructures by an electrochemically active biofilm," *Nanoscale*, vol. 5, no. 19, pp. 9238-9246, 2013, https://doi.org/10.1039/C3NR02678G.

[38] M. T. Thein, S.-Y. Pung, L. S. Chuah, and Y.-F. Pung, "Photodegradation behavior of ZnO nanorods on various types of organic dyes," *Advances in Materials and Processing Technologies*, vol. 4, no. 2, pp. 272-280, 2018, https://doi.org/10.1080/2374068X.2017.1416882.

[39] F. Chabira, M. Toubane, R. Z. Tala-Ighil, M. Humayun, S. Sagadevan, C. Ouyang, M. Bououdina, and G. Z. Kyzas, "Facile Green and Hydrothermal Synthesis of ZnO Nanorods using Eucalyptus Extract: Photocatalytic Degradation of Cationic Dye," *Water, Air, & Soil Pollution*, vol. 236, p. 334, 2025, https://doi.org/10.1007/s11270-025-07968-2.

[40] R. Vittal and K.-C. Ho, "Zinc oxide based dye-sensitized solar cells: A review," *Renewable and Sustainable Energy Reviews*, vol. 70, pp. 920-935, 2017, https://doi.org/10.1016/j.rser.2016.11.273.

[41] P. J. Mokgolo, T. P. Gumede, R. O. Ocaya, and T. D. Malevu, "Enhancing Perovskite Solar Cells With Rare-Earth Metal Doped Zinc Oxide: A Review of Electron Mobility, Stability, and Photocarrier Recombination," *International Journal of Energy Research*, vol. 2025, Art. ID 4240199, 2025, https://doi.org/10.1155/er/4240199.

[42] S. Chou, F. C. Chou, and J. Y. Kang, "Preparation of ZnO-Coated TiO2 Electrodes Using Dip Coating and Their Applications in Dye-Sensitized Solar Cells," *Powder Technology*, vol. 215-216, pp. 38-45, 2012, https://doi.org/10.1016/j.powtec.2011.09.003.

[43] W. Chen and S. Yang, "Dye-sensitized solar cells based on ZnO nanotetrapods," *Frontiers of Optoelectronics in China*, vol. 4, no. 1, pp. 24–44, 2011, https://doi.org/10.1007/s12200-011-0207-0.

[44] N. M. D. Putra, Sugianto, P. Marwoto, R. Murtafiatin, and P. D. Rizaldi, "Performance profile analysis of ZnO/CdS/CdTe solar cells thin film: A review of absorber thickness and device temperature," *Journal of Physics: Conference Series*, vol. 1567, p. 022007, 2020, https://doi.org/10.1088/1742-6596/1567/2/022007.

[45] A. Garcia-Barrientos, R. C. Ambrosio-Lazaro, R. Ramirez-Bone, M. A. Garcia-Ramirez, O. Perez-Cortes, R. Tapia-Olvera, and J. Plaza-Castillo, "pH-Effect in the Fabrication of ZnO Nanostructured Thin Films by Chemical Bath Deposition for

Increasing the Efficiency of Solar Cells," *Materials*, vol. 16, no. 8, p. 3275, 2023, https://doi.org/10.3390/ma16083275.

[46] S. Kiprotich, J. Ungula, and H. C. Swart, "Effect of Deposition Time on Material Properties of ZnO Nanorods Grown on GZO Seed Layer by CBD," *Journal of Nanosciences*, vol. 6, pp. 1-6, 2024, https://doi.org/10.47363/JNSRR/2024(6)156.

[47] Y. M. Lee, C. L., Y. T. Chen, M. H. Cai, S. Y. Liou, M. R. Zheng, J. S. Lin, and S. W. Yang, "Solid-State Dye-Sensitized Solar Cells Based on ZnO Nanorod Arrays by Low-Temperature Chemical Bath Deposition," *Advanced Materials Research*, vol. 189-193, pp. 3458-3461, 2011, https://doi.org/10.4028/www.scientific.net/AMR.189-193.3458.

نمو وتوصيف قضبان أكسيد الزنك النانوية (ZnO) المحضَّرة بطريقة الترسيب في الحمام الكيميائي لاستخدامها كأقطاب ضوئية في الخلايا الشمسية المحسَّسة بالصبغة.

نور أحمد عبدالله و باسل علي عبدالله و منال زكي رجب

قسم الفيزياء, كلية العلوم, جامعة البصرة, البصرة، العراق.

المستخلص

استُخدمت طريقة الترسيب في الحمام الكيميائي (CBD) بفعالية لإنشاء قضبان نانوية من أكسيد الزنك (ZnO) على ركائز أكسيد القصدير المشوب بالفلور (FTO)، والتي استُخدمت بعد ذلك كأقطاب ضوئية موجبة في الخلايا الشمسية المحسَّسة بالصبغة (DSSCs). تم تأكيد تكوّن طور بلوري سداسي من نوع وورتزيت مع اتجاه تفضيلي على طول المستوى (002) من خلال التوصيف البنيوي باستخدام حيود الأشعة السينية (XRD). أظهرت نتائج المجهر الألكتروني الماسح بانبعاث المجال (FE-SEM) قضباناً نانوية مصطفة عمودياً ذات مورفولوجيا منتظمة. أشار التحليل البصري باستخدام مطيافية الأشعة فوق البنفسجية–المرئية (UV-Vis) إلى انخفاض فجوة الطاقة إلى (3.27) إلكترون فولت وشفافية عالية في الطيف المرئي مقارنةً بأكسيد الزنك السائب. أظهرت الخلايا الشمسية المحسَّسة بالصبغة المُحضَّرة والمعتمدة على الأقطاب الضوئية من قضبان ZnO النانوية أنه تحت إضاءة شمسية محاكاة بكتلة هواء (AM 1.5G)، كانت كثافة التيار الضوئي (J_{sc}) تساوي 0.911 ملي أمبير/سم²، وكان عامل الامتلاء (FF) يساوي 29%، وكان جهد الدائرة المفتوحة (V_{oc}) يساوي 0.27 فولت، وكانت كفاءة تحويل القدرة (PCE) تساوي 0.07%. تشير هذه النتائج إلى أن تحضير قضبان ZnO النانوية بطريقة CBD يقدم بديلاً منخفض التكلفة واعداً للأقطاب الضوئية في الخلايا الشمسية المحسَّسة بالصبغة.

الكلمات المفتاحية: الترسيب الكيميائي في الحمام (CBD)، خلايا شمسية حساسة للصبغة، قضبان نانوية من أكسيد الزنك (NRs)، بنية نانوية من أكسيد الزنك.